Electrical Noise and Transport Properties of Graphene

Nan Sun · Kristof Tahy · Huili Xing ·
Debdeep Jena · Gerald Arnold · Steven T. Ruggiero

Abstract We present a study of the noise properties of single-layer exfoliated graphene as a function of gate bias. A tunnel/trap model is presented based on the interaction of graphene electrons with the underlying substrate. The model incorporates trap position, energy, and barrier height for tunneling into a given trap—along with the band-structure of the graphene—and is in good accord with the general characteristics of the data.

1 Introduction

The noise properties of single-layer graphene (SLG), bi-layer graphene (BLG), and multi-layer graphene (MLG) speak to the intrinsic properties of this unique materials system [1–3]. It is generally believed that, as is the case for carbon nanotubes (CNTs) [4], the traps/impurities associated with underlying oxide substrates are responsible for the low-frequency noise in graphene [5]. This assumption has been explored by noise investigations of various kinds of graphene systems [6, 7] using a variety of measurement techniques [8]. Notable is the significant noise reduction in graphene systems whose oxide substrates were removed [9, 10], or replaced by alternative high-quality crystals such as SiC [11]. Other contributing low-frequency noise sources have also been identified including gas molecules at graphene surfaces [12], electrolyte solution effects [13], electrical contacts [14, 15], lattice structural disorder [16], and processes associated sample aging [17].

N. Sun · G. Arnold · S.T. Ruggiero (✉)
Department of Physics, University of Notre Dame, Notre Dame, IN 46556, USA
e-mail: sruggier@nd.edu

K. Tahy · H. Xing · D. Jena
Department of Electrical Engineering, University of Notre Dame, Notre Dame, IN 46556, USA

An important perspective on such results has been obtained through gate-induced carrier density modulation noise studies. For BLG [18, 19] and MLG [20], the noise power scales in proportion to the gate-induced carrier density, showing a V-shaped gate dependence (a noise minimum as a function of gate potential). For SLG, two distinct noise behaviors have been observed: (i) the noise either scales as the inverse of the gate-induced carrier density, in keeping with the Hooge model [21, 22], producing a Λ-shaped gate dependence [23]; or (ii) has a V-shaped noise minimum in the vicinity of the charge-neutrality point (CNP) accompanied by two adjacent peaks (M-shaped behavior). A number of models have been proposed to explain the latter behavior. For liquid-based SLG samples an augmented charge-noise model for the observed M-shaped noise characteristics was proposed [24], where the noise amplitude is proportional to the sample transconductance, dI_{ds}/dV_g [25]. However, this approach appears unsuccessful in modeling results for vacuum-based SLG samples [26]. It has been similarly observed that the noise in SLG depends strongly on a sample's mobility, and that M-shaped noise can be successfully fit by a modified Hooge model [27]. M-shaped noise behavior has also been attributed to spatial charge inhomogeneity, where the interactions with electron and hole puddles give rise to a noise minimum at the CNP [28]. Therefore, although models for the noise associated with particular situations appear promising, a general understanding of its microscopic origin is presently lacking.

In this work we present noise results for simple, single-layer exfoliated graphene samples, and interpret the results in the context of a tunnel/trap noise model. The model assumes that carriers from the graphene layer tunnel into and out of traps in the underlying oxidized Si substrate. The model incorporates the position, energy, and barrier height of a given trap, in addition to the band-structure of the graphene. It is consistent with the Hooge result for gate biases away from the charge neutrality point, and can reproduce both Λ- and M-shaped behavior in the noise amplitude. The model provides a result in good accord with the data obtained in this study for reasonable input parameters, and as such provides an estimate for the average tunneling probability into the underlying traps.

2 Noise Measurements

We performed work on FET-like structures made from exfoliated graphene. Samples were created on electronic-grade oxidized Si substrates, using commercially prepared graphene flakes and standard e-beam lithography. As shown in Fig. 1, a large flake was patterned using an oxygen plasma to form three adjacent FET-like structures with the same sample width: $W = 5$ μm, but different sample lengths: $L_A = 4$ μm, $L_B = 6$ μm, and $L_C = 8$ μm, corresponding to samples A, B, and C, respectively. The backside of the wafer was metalized and used as a back gate to bias the devices through the ~300 nm SiO$_2$ layer. Based on transfer characteristics, the mobility for all samples was found to be ~900 cm^2/V s for holes and slightly lower for electrons. The devices exhibited on-off ratios of 4–6.

Noise measurements were conducted under vacuum inside a shielded metal probe station at 300 K. We used a simple battery-powered current source with wire-wound

Fig. 1 (**a**) Optical image of exfoliated graphene systems, samples A, B and C; and (**b**) schematic cross section of the device layout (Color figure online)
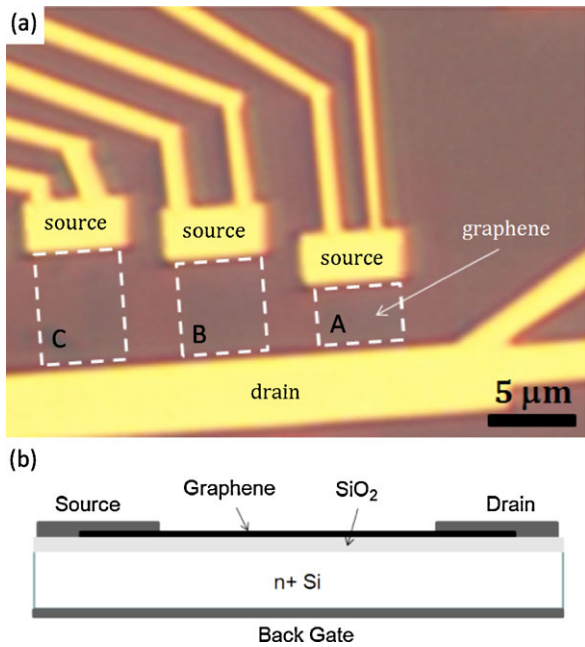
resistors and a battery-powered Princeton Applied Research PAR-113 preamplifier. The resultant amplified ac signal was sent into a Stanford Research SR760 spectrum analyzer. The background white noise from the preamplifier and Johnson noise of the sample were in the vicinity of 10^{-16} V^2/Hz, orders of magnitude below the $1/f$ noise of biased graphene samples. We found no significant difference in results using a quasi-four-point geometry, as pictured in Fig. 1, and other measurements on similarly prepared samples using an explicitly four-point configuration.

Figure 2(a) shows the observed spectral noise density (S_V) as a function of frequency for a variety of gate voltages, which generally shows a $1/f$-like behavior. The small peak appearing at 60 Hz is due to 60-Hz line pickup and does not affect our analysis. The noise amplitude can be expressed in terms of normalized voltage spectral density as

$$A_N = f^n S_V / V^2, \tag{1}$$

where n is the frequency exponent with a value typically close to unity and S_V is the spectral noise density in units of V^2/Hz^n. In Fig. 3(a), the noise amplitude A_N (here $n = 1$) is plotted as a function of gate bias, showing a maximum in the normalized noise in the vicinity of the CNP, in accord with a model assuming primary noise contributions from gated graphene elements and single rather than bi-layer films, since double-layer films appear to exhibit a normalized noise minimum at the CNP.

We first characterize the noise behavior using the empirical Hooge model. This approach invokes the parameter $\alpha_H = A_N N$, where N is the total number of charge carriers. Substituting the resistance $R = L^2 / e\mu N$, this can be re-written as

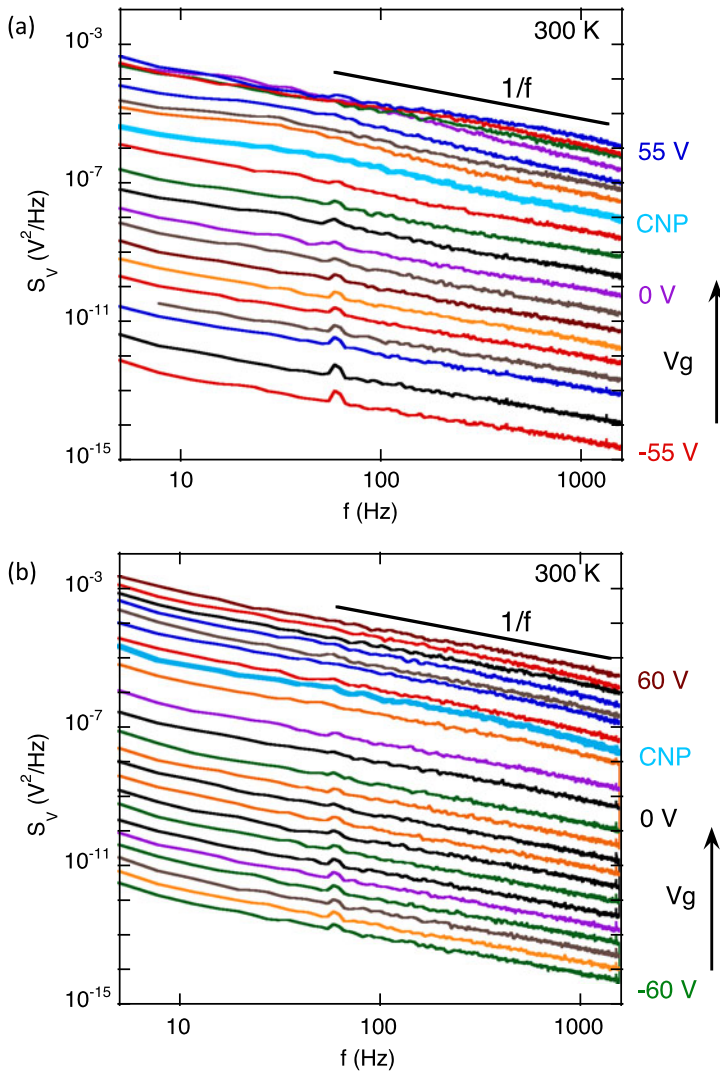$$A_N / R = (e\mu / L^2) \alpha_H, \tag{2}$$

Fig. 2 (**a**) Spectral noise density S_V of an exfoliated graphene system (sample A, Fig. 1) as a function of frequency at various gate biases. Noise spectra offset vertically from the lowest curve for clarity. (**b**) Same measurement for sample B (Color figure online)

where μ is the carrier mobility, e is the elementary charge, and L is the sample length. The dashed red curve in Fig. 3(a) is a Hooge-model fit for the noise amplitude A_N for sample A with a Hooge parameter of $\alpha_H = 0.045$, and where $R = 1/G$ is the gate-dependent sample resistance. The empirical Hooge model shows good agreement with the noise amplitude at gate biases away from the CNP (in the vicinity of 20 V gate bias) but, since the peak in the noise amplitude is offset from the minimum in sample conductance (appearing in the vicinity of 40 V gate bias), the model does not correctly reproduce the behavior of the noise peak near the CNP.
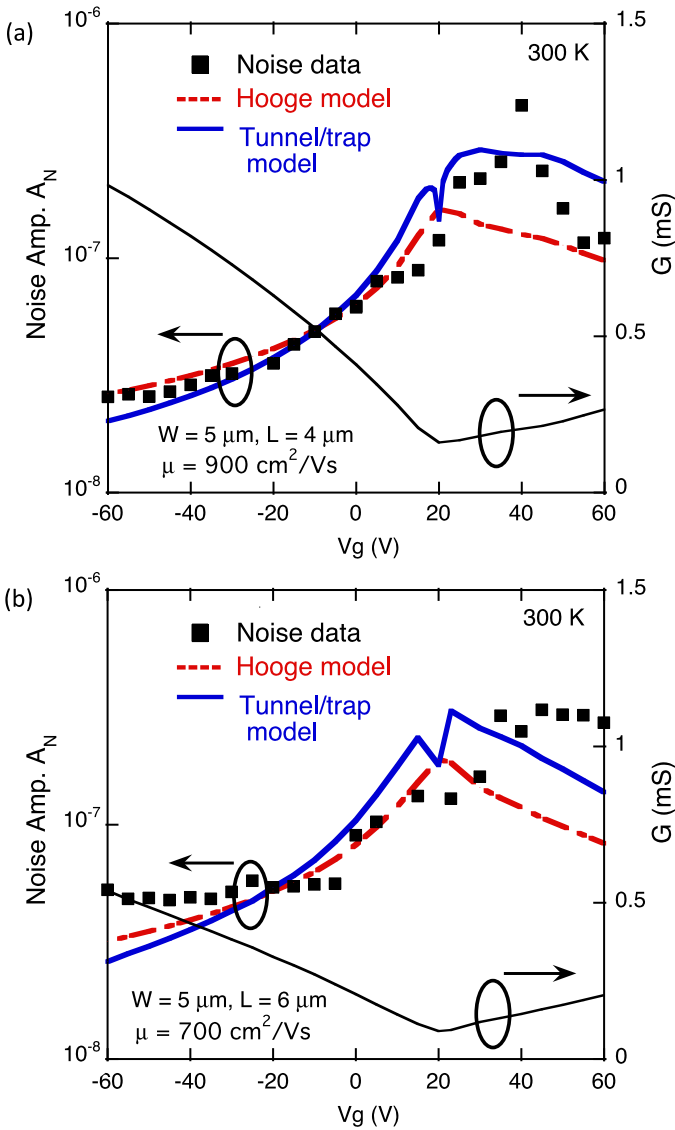
Fig. 3 (**a**) and (**b**) show the measured conductance (*solid thin line*) and the noise amplitude A_N (*solid squares*) as a function of gate voltage for graphene samples A and B, respectively (see Fig. 1). Also shown are theoretical fits from the Hooge model (*dashed red line*) and for our tunnel/trap model (*solid thick blue line*) (Color figure online)

Figure 3(b) shows the noise characteristics of an adjacent "sister" sample B as shown in Fig. 1, which are generally similar to sample A in all regards. However, we note that in the electron branch the noise amplitude forms a plateau above 40 V rather than a peak as seen in Fig. 3(a) for sample A. The dashed curve is a fit for the noise amplitude A_N with a Hooge parameter of $\alpha_H = 0.055$.

3 Tunnel/Trap Model

A generally accepted model to describe the noise originating from interfacial traps in semiconducting devices was proposed by McWhorter [22]. This model successfully describes the proportionality of the oxide-trap density to the magnitude of $1/f$ noise in MOSFET devices (at a given gate bias) [31]. Since in our and many other studies of graphene flakes and deposited films, the material lies on a Si/SiO$_2$ substrate, it is natural to assume that graphene transport measurements would likewise be susceptible to the same noise, due to tunneling transitions between interfacial oxide traps at the graphene/SiO$_2$ boundary and free electron states in the graphene [5, 23, 26].

In order to provide further insight into the nature of the generally observed noise peak in graphene, we present here a tunnel/trap noise model with a starting point that parallels the McWhorter model. As with previous models, our approach assumes that graphene films sit on a SiO$_2$ layer with a given density of electron traps, but which also now specifies a given physical distribution of traps and distribution of trap well depths. Carriers from the graphene are assumed to tunnel into the traps, become captured, and then at some point tunnel back into the graphene film, causing fluctuations in the current flow. This process will create $1/f$-like noise which is a function of the gate bias through a shift in the Fermi level of the graphene with gate bias. In this process, the number of carriers available for tunneling will be governed by the bias-dependent tunneling density of states (DOS) of the graphene. In our model, the tunneling is characterized by the following Hamiltonian:

$$H = \sum_{\vec{k},\sigma} \bar{\Psi}_{\vec{k},\sigma} [\vec{\gamma} \cdot \vec{k} - \mu] \Psi_{\vec{k},\sigma} + \sum_{\vec{k},\sigma,i} [V_{i,\vec{k}} \bar{D}_{i,\sigma} \Psi_{\vec{k},\sigma} + h.c.]$$
$$+ \sum_{i,\sigma} E_i \bar{D}_{i,\sigma} D_{i,\sigma}, \tag{3}$$

where μ is the gate-dependent chemical potential, and $\vec{\gamma} = (\gamma_x, \gamma_y)$, with γ^μ the four gamma matrices in the Weyl representation. Since the momentum $\vec{k}$ only has x and y components, the product $\vec{\gamma} \cdot \vec{k}$ only involves γ^1 and γ^2, where

$$\gamma^1 = \begin{pmatrix} 0 & 0 & 0 & -1 \\ 0 & 0 & -1 & 0 \\ 0 & 1 & 0 & 0 \\ 1 & 0 & 0 & 0 \end{pmatrix} \quad \text{and} \quad \gamma^2 = \begin{pmatrix} 0 & 0 & 0 & i \\ 0 & 0 & -i & 0 \\ 0 & -i & 0 & 0 \\ i & 0 & 0 & 0 \end{pmatrix}. \tag{4}$$

The first term of the Hamiltonian represents the graphene self-energy. We have

$$\bar{\Psi}_{\vec{k},\sigma} = \Psi_{\vec{k},\sigma}^+ \gamma^0 = \begin{pmatrix} a_\sigma^+(\vec{K}_+ + \vec{k}) \\ b_\sigma^+(\vec{K}_+ + \vec{k}) \\ b_\sigma^+(\vec{K}_- + \vec{k}) \\ a_\sigma^+(\vec{K}_- + \vec{k}) \end{pmatrix} \begin{pmatrix} 0 & 0 & 1 & 0 \\ 0 & 0 & 0 & 1 \\ 1 & 0 & 0 & 0 \\ 0 & 1 & 0 & 0 \end{pmatrix}, \tag{5}$$

where the operator $a_\sigma^+(\vec{K}_+ + \vec{k})$ creates an electron at an "a" site on the lattice, with spin σ and momentum $\vec{K}_+ + \vec{k}$, and the operator $b_\sigma^+(\vec{K}_+ + \vec{k})$ creates an electron at a "b" site on the lattice. $\vec{K}_+$ and $\vec{K}_-$ are the locations of two inequivalent Dirac cones in the Brillouin Zone.

The second term of the Hamiltonian represents the interaction between the graphene sheet and the traps, and the third term represents the self-energy of the traps. The operator

$$\bar{D}_{i,\sigma} = \begin{pmatrix} d_{i,\sigma}^+ \\ d_{i,\sigma}^+ \\ d_{i,\sigma}^+ \\ d_{i,\sigma}^+ \end{pmatrix} \gamma^0 \tag{6}$$

creates an electron in a trap, located adjacent to a graphene lattice site at $\vec{R}_i$. This can be an "a" or a "b" site. Since these sites are otherwise physically equivalent, and since $\vec{R}_i$ is a random variable, we enter both kinds of sites on an equal footing.

The local energy, E_i, is also a random variable, as is the matrix element for transfer into the trap, $V_{i,\vec{k}}$, which we take to be an exponential function of a (dimensionless) random barrier potential, μ_i, as $V_{i,\vec{k}} = Q_{i,\vec{k}} e^{-\mu_i}$.

Assuming a probability distribution $P(\vec{R}_i)$ for the trap position, $P(E_i)$ for the trap energy, and $P(\mu_i)$ for the tunnel barrier height, we make the approximation that the probability distribution for each variable is separable as:

$$P(\vec{R}_i, \mu_i, E_i) = P(\vec{R}_i) P(\mu_i) P(E_i). \tag{7}$$

The noise is calculated using the current-current correlation function [29]. For each trap state, the noise spectrum is given by:

$$S_V(\omega) = \alpha \frac{e^2}{\pi} \int d\varepsilon \frac{1}{\sigma^2(V_g)} \left[\frac{|\tilde{\varepsilon}|\Gamma_\omega}{\omega^2 + \Gamma_\omega^2} + \frac{|\tilde{\varepsilon}_\omega|\Gamma}{\omega^2 + \Gamma^2} \right] [1 - F(\varepsilon)F(\varepsilon + \omega)], \tag{8}$$

where α is the sample geometrical aspect ratio, e is the electron charge, ε is the electron energy, $\sigma(V_g)$ is the conductivity as a function of the gate voltage, Γ is the scattering rate, and $F(\varepsilon) = \tanh(\varepsilon/2k_B T)$. This expression gives a Lorentzian spectrum, and must be averaged over the appropriate random variables (Eq. (7)), finally yielding a $1/f$-like spectrum. The averaged power spectral density is given as

$$\langle S_V(\omega) \rangle = k \left(\frac{f_0}{f} \right) \frac{\sigma_{\min}^2}{\sigma^2(V_g)} (|\mu| + a_{\min}), \tag{9}$$

where the prefactor k is a fitting parameter, the implication of which will be discussed later, f_0 is a normalization constant taken here as the noise measurement frequency of 100 Hz, σ is the conductivity, and $a_{\min} = 4k_B T \ln 2 = 66.5$ meV at 300 K.

The averaged power spectral density $\langle S_V \rangle$ of the noise in Eq. (9) will thus typically reflect the product between a peak in the normalized conductance $\sigma_{\min}^2/\sigma^2(V_g)$ with gate voltage, V_g, and a sharp dip in the chemical potential. The dip in the chemical potential as a function of gate voltage arises from the fact that the DOS is taken to be proportional to the Fermi energy as $D(E_F) \propto |E_F|$, and we make the usual assumptions that $\mu = E_F$, and that $E_F \propto \sqrt{|V_g - V_{CNP}|}$, where V_{CNP} is the gate bias voltage at the CNP, whereby we have a square-root-like dip in the chemical potential at the CNP. Thus, the noise power is expected to have an overall M-shaped power spectral density, whereas Λ-shaped results represent the case where this DOS-related effect is not prominent. We note that our assumed correlation between noise behavior and DOS is consistent with earlier studies on graphene nanoribbons [30].

4 Discussion

In Fig. 3(a) and (b) we have applied this noise model to our measured results for samples A and B, respectively. Here we have used the normalized conductance measurements for each sample and an idealized model for the variation in the chemical potential with gate bias. The model is generally consistent with the phenomenological Hooge model away from the CNP, and shows finer structure which parallels measured variations of A_N in the vicinity of the noise peak. The model also better represents the offset of the noise peak from the CNP. Note that the sharpness in the dip predicted by theory is an artifact of the idealized functional dependence of the chemical potential used in the calculation.

We can also use the model to extract specific information about the nature of the trap system itself. From the calculation, the prefactor k is given by

$$k = \frac{\alpha \pi C_{av} S_J(T)}{h f_0},$$ (10)

where $\alpha = W/L = 1.25$ is the geometrical aspect ratio for sample A, h is the Plank's constant, $S_J(300 \text{ K}) = 4 k_B T R = 3.2 \times 10^{-17} \text{ V}^2/\text{Hz}$ is the Johnson noise, $f_0 = 100$ Hz, and C_{av} is a dimensionless constant which represents an average tunneling rate into the traps. The best fits to the data for sample A was for a value of $k = 2.2 \times 10^{-8} \text{ eV}^{-1} \text{ Hz}^{-1}$. From this we find a value of $C_{av} = 7.24 \times 10^{-5}$. If we assume a typical defect density of 10^{12} cm^{-2} [31–33], the average distance between two traps is

$$d = \sqrt{\frac{1}{10^{12} \text{ cm}^{-2}}} = 10 \text{ nm}.$$ (11)

For graphene, we also know that within a $10 \times 10 \text{ nm}^2$ area there are 3.8×10^3 carbon atoms [34]. Thus the fractional density of traps is equal to

$$D = \frac{1}{3.8 \times 10^3} = 2.6 \times 10^{-4}.$$ (12)

We can finally define a scattering probability

$$p = \frac{C_{av}}{D} = \frac{7.24 \times 10^{-5}}{2.6 \times 10^{-4}} = 27.8 \text{ \%}.$$ (13)

This is the average scattering probability (per attempt) per defect. This can be translated into an estimated mean-free path for sample A as:

$$l_{mfp} \sim d/p = \frac{10 \text{ nm}}{0.278} = 36 \text{ nm}.$$ (14)

We find a similar result of 29 nm for the mean-free path for sample B. These values are in accord with a mean-free path of graphene generally believed to be $\sim$50–60 nm for a defect density of $\sim 10^{12} \text{ cm}^{-2}$ [35]. We note finally that charge transport in graphene is diffusive if the defect density is in the vicinity of our assumed value of 10^{12} cm^{-2}. This is consistent with charge scattering primarily due to long-range Coulomb scattering (i.e., from charged impurities), rather than short-range scattering (i.e., from lattice defects) [36].

5 Conclusions

Noise measurements of single-layer graphene have revealed interesting phenomenology in this system, especially in the vicinity of the charge neutrality point (CNP). The offset of a broad noise peak from the CNP, the noise asymmetry in the electron/hole branches, and a distinct dip observed in the noise within a broader noise peak, are in accord with a tunnel/trap model proposed here.

References

1. K.S. Novoselov, A.K. Geim, S.V. Morozov, D. Jiang, Y. Zhang, S.V. Dubonos, I.V. Grigorieva, A.A. Firsov, Electric field effect in atomically thin carbon films. Science **306**, 666–669 (2004)
2. S. Das Sarma, S. Adam, E.H. Hwang, E. Rossi, Electronic transport in two-dimensional graphene. Rev. Mod. Phys. **83**, 407–470 (2011)
3. P. Avouris, Graphene: electronic and photonic properties and devices. Nano Lett. **10**, 4285–4294 (2010)
4. Y.-M. Lin, J. Appenzeller, J. Knoch, Z. Chen, P. Avouris, Low-frequency current fluctuations in individual semiconducting single-wall carbon nanotubes. Nano Lett. **6**, 930–936 (2006)
5. Y.-M. Lin, P. Avouris, Strong suppression of electrical noise in bilayer graphene nanodevices. Nano Lett. **8**, 2119–2125 (2008)
6. G. Xu, J. Bai, C.M. Torres, Jr., E.B. Song, J. Tang, Y. Zhou, X. Duan, Y. Zhang, K.L. Wang, Low-noise submicron channel graphene nanoribbons. Appl. Phys. Lett. **97**, 073107 (2010)
7. A.N. Pal, A.A. Bol, A. Ghosh, Large low-frequency resistance noise in chemical vapor deposited graphene. Appl. Phys. Lett. **97**, 133504 (2010)
8. M.G. Sung, H. Lee, K. Heo, K.-E. Byun, T. Kim, D.H. Seo, S. Seo, S. Hong, Scanning noise microscopy on graphene devices. ACS Nano **5**, 8620–8628 (2011)
9. Z. Cheng, Q. Li, Z. Li, Q. Zhou, Y. Fang, Suspended graphene sensors with improved signal and reduced noise. Nano Lett. **10**, 1864–1868 (2010)
10. X. Du, I. Skachko, A. Barker, E.Y. Andrei, Approaching ballistic transport in suspended graphene. Nat. Nanotechnol. **3**, 491–495 (2008)
11. J.S. Moon, D. Curtis, D. Zehnder, S. Kim, D.K. Gaskill, G.G. Jernigan, R.L. Myers-Ward, C.R. Eddy Jr., P.M. Campbell, K.-M. Lee, P. Asbeck, Low-phase-noise graphene FETs in ambipolar RF applications. IEEE Electron Device Lett. **32**, 270–272 (2011)
12. S. Rumyantsev, G. Liu, M.S. Shur, R.A. Potyrailo, A.A. Balandin, Selective gas sensing with a single pristine graphene transistor. Nano Lett. **12**, 2294–2298 (2012)
13. M. Dankerl, M.V. Hauf, A. Lippert, L.H. Hess, S. Birner, I.D. Sharp, A. Mahmood, P. Mallet, J.-Y. Veuillen, M. Stutzmann, J.A. Garrido, Graphene solution-gated field-effect transistor array for sensing applications. Adv. Funct. Mater. **20**, 3117–3124 (2010)
14. Q. Shao, G. Liu, D. Teweldebrhan, A.A. Balandin, S. Rumyantsev, M. Shur, D. Yan, Flicker noise in bilayer graphene transistors. IEEE Electron Device Lett. **30**, 288–290 (2009)
15. G. Liu, W. Stillman, S. Rumyantsev, Q. Shao, M. Shur, A.A. Balandin, Low-frequency electronic noise in the double-gate single-layer graphene transistors. Appl. Phys. Lett. **95**, 033103 (2009)
16. K. Kim, H.J. Park, B.-C. Woo, K.J. Kim, G.T. Kim, W.S. Yun, Electric property evolution of structurally defected multilayer graphene. Nano Lett. **8**, 3092–3096 (2008)
17. S. Rumyantsev, G. Liu, W. Stillman, M. Shur, A.A. Balandin, Electrical and noise characteristics of graphene field-effect transistors: ambient effects, noise sources and physical mechanisms. J. Phys. Condens. Matter **22**, 395302 (2010)
18. A.N. Pal, A. Ghosh, Resistance noise in electrically biased bilayer graphene. Phys. Rev. Lett. **102**, 126805 (2009)
19. A.N. Pal, A. Ghosh, Resistance noise in graphene based field effect devices. AIP Conf. Proc. **1129**, 479–482 (2009)

20. A.N. Pal, A. Ghosh, Ultralow noise field-effect transistor from multilayer graphene. Appl. Phys. Lett. **95**, 082105 (2009)
21. F.N. Hooge, $1/f$ noise sources. IEEE Trans. Electron Devices **41**, 1926–1935 (1994)
22. F.N. Hooge, T.G.M. Kleinpenning, L.K.J. Vandamme, Experimental studies on $1/f$ noise. Rep. Prog. Phys. **44**, 479–532 (1981)
23. A.N. Pal, S. Ghatak, V. Kochat, E.S. Sneha, A. Sampathkumar, S. Raghavan, A. Ghosh, Microscopic mechanism of $1/f$ noise in graphene: role of energy band dispersion. ACS Nano **5**, 2075–2081 (2011)
24. J. Tersoff, Low-frequency noise in nanoscale ballistic transistors. Nano Lett. **7**, 194–198 (2007)
25. I. Heller, S. Chatoor, J. Mannik, M.A.G. Zevenbergen, J.B. Oostinga, A.F. Morpurgo, C. Dekker, S.G. Lemay, Charge noise in graphene transistors. Nano Lett. **10**, 1563–1567 (2010)
26. A.A. Kaverzin, A.S. Mayorov, A. Shytov, D.W. Horsell, Impurities as a source of $1/f$ noise in graphene. Phys. Rev. B **85**, 075435 (2012)
27. Y. Zhang, E.E. Mendez, X. Du, Mobility-dependent low-frequency noise in graphene field-effect transistors. ACS Nano **5**, 8124–8130 (2011)
28. G. Xu, C.M. Torres, Jr., Y. Zhang, F. Liu, E.B. Song, M. Wang, Y. Zhou, C. Zeng, K.L. Wang, Effect of spatial charge inhomogeneity on $1/f$ noise behavior in graphene. Nano Lett. **10**, 3312–3317 (2010)
29. A. Golub, B. Horovitz, Shot noise in graphene with long-range Coulomb interaction and local Fermi distribution. Phys. Rev. B **81**, 245424 (2010)
30. G. Xu, C.M. Torres, Jr., E.B. Song, J. Tang, J. Bai, X. Duan, Y. Zhang, K.L. Wang, Enhanced conductance fluctuation by quantum confinement effect in graphene nanoribbons. Nano Lett. **10**, 4590–4594 (2010)
31. R. Jayaraman, C.G. Sodini, A $1/f$ noise technique to extract the oxide trap density near the conduction band edge of silicon. IEEE Trans. Electron Devices **36**, 1773–1782 (1989)
32. S. Adam, E.H. Hwang, V.M. Galitski, S. Das Sarma, A self-consistent theory for graphene transport. Proc. Natl. Acad. Sci. USA **104**, 18392–18397 (2007)
33. T. Ando, A.B. Fowler, F. Stern, Electronic properties of two-dimensional systems. Rev. Mod. Phys. **54**, 437–672 (1982)
34. A.H. Castro Neto, F. Guinea, N.M.R. Peres, K.S. Novoselov, A.K. Geim, The electronic properties of graphene. Rev. Mod. Phys. **81**, 109–162 (2009)
35. J.-H. Chen, W.G. Cullen, C. Jang, M.S. Fuhrer, E.D. Williams, Defect scattering in graphene. Phys. Rev. Lett. **102**, 236805 (2009)
36. C. Jang, S. Adam, J.-H. Chen, E.D. Williams, S. Das Sarma, M.S. Fuhrer, Tuning the effective fine structure constant in graphene: opposing effects of dielectric screening on short- and long-range potential scattering. Phys. Rev. Lett. **101**, 146805 (2008)